

A first-principles investigation of altermagnetism in CrSb₂ under applied pressure

R. Tamang,^{1,2} Shivraj Gurung,² Shalika Ram Bhandari,³ Matthew J. Stitz,⁴ Ganesh Pokharel,⁴ Keshav Shrestha,⁵ and D. P. Rai¹

¹*Department of Physics, Mizoram University, Aizawl-796004, India*

²*Physical Sciences Research Center (PSRC), Department of Physics, Pachhunga University College, Aizawl-796001, India*

³*Department of Physics, Bhairahawa Multiple Campus, Tribhuvan University, Nepal*

⁴*Perry College of Mathematics, Computing, and Sciences, University of West Georgia, Carrollton, GA 30118, USA*

⁵*Department of Chemistry and Physics, West Texas A&M University, Canyon, Texas 79016, USA*

(Dated: June 17, 2025)

In this study, we employed first-principles density functional theory (DFT) calculations within the GGA+U framework to explore the electronic and magnetic properties of CrSb₂ under varying hydrostatic pressures. CrSb₂ exhibits non-relativistic spin splitting (NRSS) of ~ 0.5 eV around the Fermi level and the d -wave symmetric Fermi surface. Our magnetic susceptibility measurements further confirm the collinear antiferromagnetic (AFM) ground state in CrSb₂, a prerequisite for altermagnetism. The presence of collinear AFM and spin-band splitting without the application of spin-orbit coupling (SOC) supports CrSb₂ as a potential contender for altermagnet. With increasing pressure, we have observed an intricate evolution of spin splitting in the valence and conduction bands, governed by changes in orbital contributions. The observation of the structural phase transition above 10 GPa is in qualitative agreement with the previous experimental findings. Our results not only support the classification of CrSb₂ as an altermagnetic candidate but also provide critical insight into the role of pressure in tuning its spin-dependent electronic structure.

I. INTRODUCTION

In recent years, altermagnets (AMs), a newly identified magnetic material, have garnered significant attention in the scientific community, evidenced by the publication of several hundred research articles on the topic. AMs combine essential features of antiferromagnets (AFMs), such as compensated collinear magnetic ordering, and ferromagnets (FMs), including time-reversal symmetry (\mathcal{T}) breaking and lifting Kramer's degeneracy in the band structures without relativistic spin-orbit coupling (SOC). However, they exhibit distinct symmetries that separate them from both AFM and FM^{50,51}. In traditional collinear AFMs, the symmetry that connects the two opposite spin sublattices is \mathcal{T} combined with parity (P) or transition (t). However, in altermagnets (AMs), due to the specific crystal environment around each magnetic atom, the opposite spin sublattices are related by rotations, screws, glide, and mirrors⁵² the opposite spin sublattices are related by rotations in both spin and real space followed by translation [see Fig.1(b)]. While FMs are prone to stray fields, which can cause device malfunctions⁵. On the other hand, AFMs lack spin polarization. In this context, AMs emerge by leveraging the advantages of both conventional magnetic phases, FMs and AFMs, while exhibiting non-relativistic spin splitting (NRSS) in their band structure, concurrently achieving immunity to stray magnetic fields.^{35,50,51} NRSS is comparable to the spin-splitting induced by relativistic SOC on the order of a few electron volts^{50,51}.

First-principles calculations have identified several bulk and two-dimensional materials as potential altermagnets with distinct NRSS^{3,22,51}. However, only a few

materials have been experimentally confirmed to exhibit NRSS, as investigated through angle-resolved photoemission spectroscopy (ARPES)^{12,28,44,57,60}. Various spin-dependent phenomena can emerge in this novel magnetic phase. Notably, the anomalous Hall effect (AHE), traditionally considered forbidden in collinear antiferromagnets due to the preservation of time-reversal symmetry (\mathcal{T}), has recently garnered significant attention. Anomalous Hall conductivity represents a dissipationless portion of the conductivity tensor⁴⁷. Contrary to conventional understanding, theoretical predictions indicated the possibility of AHE in collinear antiferromagnetic RuO₂, a finding that has been experimentally validated in altermagnetic RuO₂^{16,55}. Subsequent experimental confirmations of AHE have been reported in other altermagnetic materials, including Mn₅Si₃^{29,43}, MnTe^{20,26}, and CrSb⁵⁹. These observations collectively confirm the spontaneous breaking of \mathcal{T} -symmetry in AMs. Additionally, altermagnets (AMs) exhibit significant potential for spintronic applications, owing to the generation of spin currents^{7,21,37,38,46}, giant and tunnel magnetoresistance effects^{9,10,24,34,48}, spin-splitter torques^{2,25}, efficient spin-to-charge conversion^{1,58}, and ultrafast magnetic dynamics operating in the terahertz (THz) regime^{4,49}. These phenomena position AMs as highly promising candidates for next-generation spintronic technologies⁵².

Various theories have been developed to describe AM, with one prominent theory utilizing the spin group theory developed by Litvin et al.^{32,33}, which has been applied to explain the NRSS in AM.⁵⁰ Radaelli and group used the tensorial approach to discuss altermagnetism⁴². Bhowal et al.⁶ investigated the centrosymmetric antiferromagnet MnF₂, emphasizing

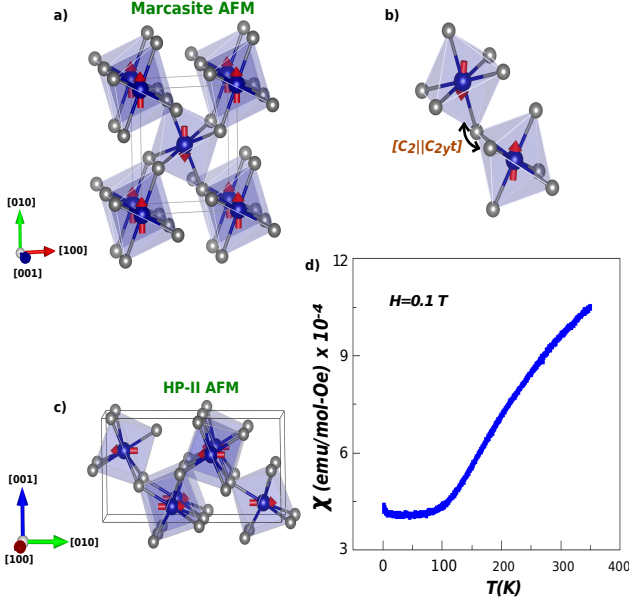


FIG. 1. a) The unit cell structure of CrSb_2 , with magnetic Cr atoms depicted in blue and non-magnetic atoms in grey. b) The opposite spin sublattices are related by a two-fold rotation in both spin space and real space, $([C_2|C_{2yt}])$, followed by a half-unit-cell translation. c) HP-II AFM phase of CrSb_2 . (d) Magnetic susceptibility (χ) as a function of temperature measured under an applied field of $H = 0.1$ T for the marcasite- CrSb_2 . The susceptibility $\chi(T)$ decreases with decreasing temperature, exhibiting behavior consistent with antiferromagnetism, with a Neel temperature above room temperature.

the role of higher-order multipoles in driving NRSS. Magnetic octupoles in MnF_2 break time-reversal symmetry and induce NRSS without relying on relativistic SOC. The spin-splitting energy depends on structural and magnetic modifications, exhibiting a strong correlation with ferroic octupolar ordering. The magnitude of spin splitting can be represented by an equation

$$E(\mathbf{k}, \uparrow) - E(\mathbf{k}, \downarrow) = F(k) \sin(k_x a) \sin(k_y a)^{36}$$

Here, $F(k)$ is a k -dependent function, whereas a is the lattice constant. At high-symmetry points in the Brillouin zone, where $k_x = n\pi/a$ and $k_y = n\pi/a$ ($n=0,1,\dots$), the spin splitting vanishes, resulting in degenerate band structures along high-symmetry paths.

Although CrSb_2 has been predicted AM candidate³ but there are no solid works on the presence of altermagnetism in CrSb_2 . Moreover, altermagnetism has already been reported in its close cousins like CrSb ^{12,44,56} and FeSb_2 ⁴¹. The experimental studies have confirmed the marcasite AFM structure of CrSb_2 at ambient pressure²³, analogous to that of FeSb_2 , along with the observation of comparable Seebeck coefficients⁴⁵. Experimentally, the existence of altermagnetism in FeSb_2 has already been

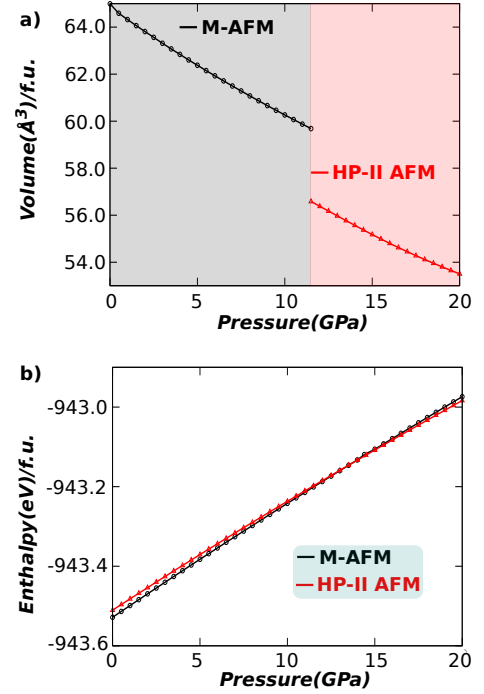


FIG. 2. a) Variation of volume per formula unit(f.u.) with applied pressure in both marcasite(M) and HP-II phase of antiferromagnetic CrSb_2 . b) Enthalpy per formula unit(f.u.) vs. pressure curve with crossover point above 10 GPa. The HP-II phase is thermodynamically more favourable above 10 GPa.

confirmed via Fermi surface mapping⁴¹. Complementary to this, the surface properties of CrSb_2 have also been extensively investigated^{13,39} and reported a pronounced surface anisotropic magnetoresistance based on angle-dependent magnetoresistance measurements. Furthermore, Mazin and colleagues have reported the presence of an anti-Kramers (AK) nodal surface alongside notable NRSS in Cr doped FeSb_2 ; such an AK nodal surface gives rise to a significant anomalous Hall conductivity (~ 150 S/cm), as demonstrated through first-principles calculations³⁶.

We have successfully grown high-quality single crystals of CrSb_2 using a conventional flux-growth method. The temperature-dependent magnetic susceptibility (χ) calculation of CrSb_2 revealed an AFM ground state. Motivated by the experimental results, we intend to perform the first-principles DFT calculation to explore the possible occurrence of altermagnetism in CrSb_2 . First-principles calculations based on density functional theory (DFT) provide a fundamental framework for probing the structural, electronic, and magnetic characteristics of materials. These computational approaches are indispensable for elucidating underlying microscopic mechanisms, rationalizing experimental findings, and systematically examining material responses to external perturbations such as pressure or strain^{8,11,15}. They play a

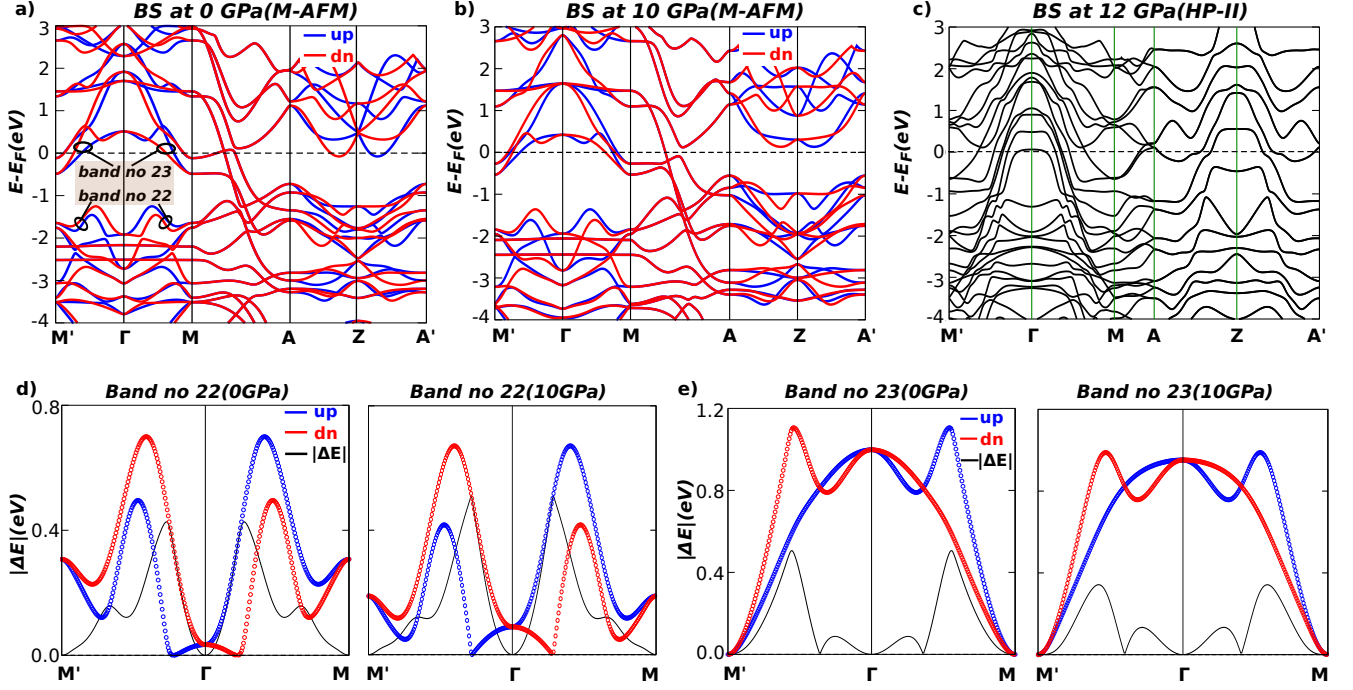


FIG. 3. Illustration of the Electronic Properties at 0, 10, and 12 GPa: (a-c) marcasite(M) AFM AT 0 GPa, M-AFM at 10 GPa, and HP-II AFM at 12 GPa, respectively. d) Amplification of the NRSS, denoted by $|\Delta E|$, is observed in band index 22 over the pressure range of 0 to 10 GPa. e) In contrast, a significant suppression of NRSS $|\Delta E|$ is evident in band index 23 within the same pressure interval.

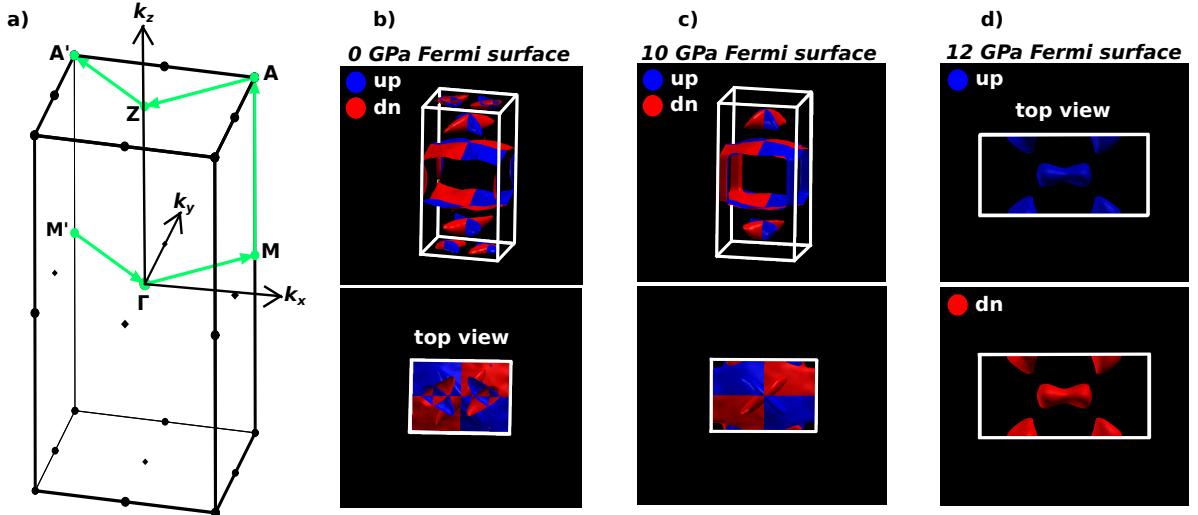


FIG. 4. Fermi surfaces under varying pressures: a) High-symmetry K-path. (b-c) Fermi surfaces at 0 and 10 GPa, respectively, depicting spin-momentum locking with characteristic d-wave symmetry in the marcasite phase. (d) Fermi surface at 12 GPa in the HP-II phase, showing symmetric spin-up and spin-down channels, confirming the absence of NRSS.

pivotal role in accelerating the rational design and discovery of novel functional materials. Furthermore, by substantially minimizing reliance on iterative experimental trial-and-error, these methods markedly enhance the efficiency and precision of materials research. Notably,

the discovery and conceptual development of altermagnetism were initially driven by insights gained through first-principles computations^{50,51}. Consequently, we analyze how hydrostatic pressure influences the electronic and magnetic properties of the system at 0K, uncover-

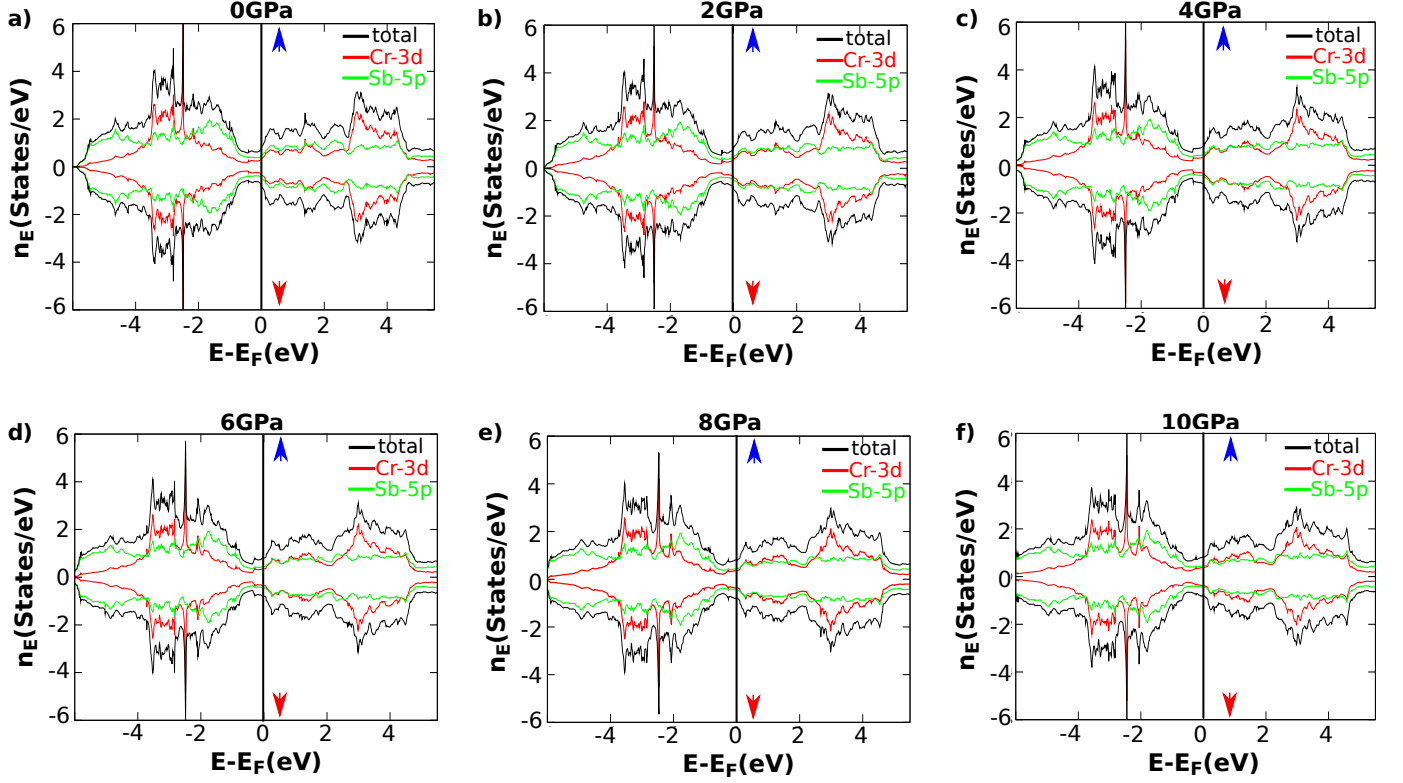


FIG. 5. Projected Density of States (PDOS) Under Varying Pressure Conditions: a)-f) Spin-resolved PDOS at 0, 2, 6, 8, and 10 GPa, respectively, demonstrating the progressive modification of the projected density of states under applied pressure.

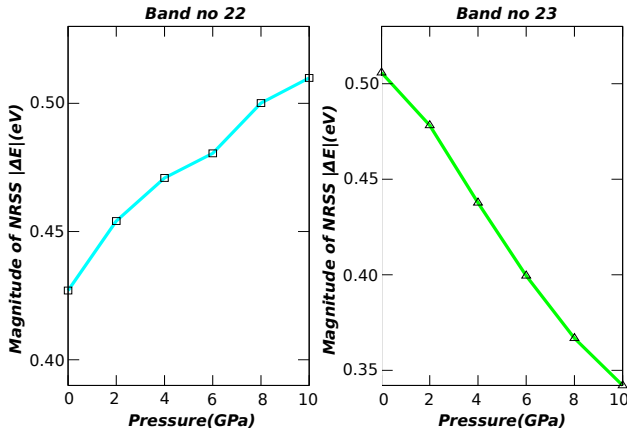


FIG. 6. Variation of spin splitting under applied pressure in the range of 0 to 10 GPa for band indices 22 and 23.

ing a strong coupling between pressure-induced structural phase transitions and the onset of altermagnetic behaviour. Our findings highlight the role of lattice compression in modulating spin-dependent band structures. A comprehensive first-principles investigation by Kuhn et al.²⁷ examined various magnetic configurations, including nonmagnetic, ferromagnetic, and antiferromagnetic

phases, to elucidate the material's electronic and magnetic ground state. The incorporation of electron correlation effects through the GGA+U approach yields results that align well with experimental findings, precisely capturing the antiferromagnetic ground state of CrSb₂.

II. METHODOLOGY

A. Sample Synthesis and Details

High-quality single crystals of CrSb₂ were grown using a conventional flux-growth technique. A self-flux of antimony (Sb) was employed to create a liquid environment conducive to initiating the solid-state reaction at high temperatures. A mixture of chromium (Cr, pieces, 99.99%) and antimony (Sb, shot, 99.9999%), both purchased from Alfa Aesar, was prepared in a molar ratio of 1:12 and loaded into a Canfield crucible set. The crucible was then sealed inside a quartz tube under an argon atmosphere at approximately 1/3 atm. The sealed ampoule was heated at a rate of 200 °C/h to 1000 °C and held at this temperature for 36 hours to ensure proper homogenization. It was then slowly cooled to 640 °C at a rate of 2 °C/h. At 640 °C, shiny CrSb₂ single crystals with typical dimensions of approximately 2 × 2 × 1

mm³ were separated from the remaining Sb flux using a centrifuge technique. The structural quality of the crystals was verified using powder X-ray diffraction (XRD) of ground crystals, and their chemical composition was examined via energy-dispersive X-ray spectroscopy (EDS) on single crystals. Magnetization measurements on the CrSb₂ single crystal were performed using a Magnetic Property Measurement System (MPMS, Quantum Design).

B. Computational Details

We have performed plane wave-based density functional theory (DFT) calculations using the open-source software package Quantum ESPRESSO^{17–19} (QE) to investigate the electronic and magnetic properties of CrSb₂. The unit cell structure, obtained from the online database The Materials Project, was optimized using the vc-relax approach. The antiferromagnetic ground state was achieved using a fine Monkhorst-Pack k-point mesh of 16×16×16. The marcasite structure of CrSb₂ with motif-pair anisotropy and AFM coupling between two opposite spin Cr atoms is shown in Fig.1(a-c). To investigate the NRSS in CrSb₂, we used ultrasoft non-relativistic pseudopotentials from the PSLibrary and PBEsol exchange correlation function⁴⁰. Furthermore, the total energy convergence was achieved with a threshold of 10⁻⁸ Rydberg. Within the GGA+*U* formalism, an on-site Hubbard *U* = 2.7 eV was assumed for the Cr 3*d* orbitals to account for correlation effects²⁷. We used energy cutoffs of 70 Ry and 750 Ry for the wave function and charge density, respectively. Hydrostatic pressure, as implemented in QE, was sequentially applied in the range of 0 to 20 GPa. To study the dynamical stability of an optimised structure 2×2×2 q-point was set for phonon dispersion calculations.

III. DISCUSSION

Figure 1(d) shows the temperature dependence of magnetic susceptibility (χ) for a CrSb₂ single crystal measured with an applied magnetic field of $H = 0.1$ T along the *c*-axis. The $\chi(T)$ curve decreases as the temperature is lowered, strongly indicating an antiferromagnetic ground state below 350 K. The Neel temperature is therefore expected to be above 350 K, beyond the experimental temperature range. Fig.1a illustrates the marcasite phase of CrSb₂, which crystallizes in the orthorhombic space group *Pnnm* (No. 58), comprises six atoms per unit cell with fully compensated magnetic moments. In this structure, Cr atoms occupy the 2a Wyckoff position, whereas Sb atoms reside at the 4g Wyckoff site¹⁴. The Sb octahedra surrounding the magnetic Cr atoms are structurally inequivalent to those surrounding the opposite-spin Cr atoms. This asymmetry gives rise to a screw sym-

metry operation that connects the two opposite spin octahedra, favoring the formation of altermagnetic order.

Under high-pressure conditions, a notable suppression of the unit cell volume is observed as shown in Fig.2a). This trend aligns well with the first-principles and experimental results^{14,30}. At 0 GPa, the optimized lattice parameters of marcasite phase are found to be $a=6.026\text{\AA}$, $b=6.846\text{\AA}$, and $c=3.151\text{\AA}$, which corresponds to a unit cell volume of 129.991 \AA^3 . This computed volume shows good agreement with the experimental value of 130.7 \AA^3 , reported in Ref.³⁰. The application of pressure modulates the lattice environment and leads to notable changes in the lattice parameters of CrSb₂. The variations of lattice parameters under the investigated pressure range (0–10 GPa) are depicted in the supplementary material, Figure S1. As pressure increases, CrSb₂ undergoes two sequential structural phase transitions. The first occurs above 5.5 GPa, where the system transforms into a CuAl₂-type structure (HP-I)⁵³. Beyond 10 GPa, a further transition leads to a MoP₂-type phase (HP-II)¹⁴. The transition is substantiated by first-principles calculations, wherein the enthalpy-pressure curves exhibit well-defined crossover points above 10 GPa at the transition pressures (illustrated in Fig. 2b). The computed phase stability trends demonstrate good agreement with experimental findings, thereby reinforcing the reliability of the theoretical approach in capturing the structural evolution of CrSb₂ under a high-pressure regime. At approximately 12 GPa, the optimized lattice parameters for the HP-II phase are $a = 2.978\text{\AA}$, $b = 12.617\text{\AA}$, and $c = 6.002\text{\AA}$, yielding axial ratios of $a/b = 0.236$ and $a/c = 0.496$. These values closely match experimental data for the MoP₂¹⁴. Due to its ferromagnetic ordering, the HP-I phase of CrSb₂ was excluded from this study⁵³. Additionally, the electronic properties also evolve under applied pressure (see Fig. 3). The electronic band structure reveals a maximum spin splitting $E(k,\uparrow) - E(k,\downarrow)$ of approximately 0.5 eV along the $M' - \Gamma - M$ path, near the Fermi level (shown in Fig. 3e) at 0 GPa). First-principles computations without the inclusion of relativistic effects underscore the potential of CrSb₂ as a candidate AM. Notably, our results demonstrate the emergence of alternating spin-momentum locking exhibiting *d*-wave symmetry, as illustrated in Fig. 4(b-c). The presence of such anti-Kramers nodal surfaces and nontrivial electronic states is indicative of the generation of a finite anomalous Hall conductivity, even in the absence of net magnetization³⁶. However, the HP-II phase of CrSb₂ exhibits no spin-momentum locking, as the spin-up and spin-down channel Fermi surfaces are completely symmetric (as shown in Fig.4d), consistent with the absence of NRSS in the HP-II phase. Fig.5 illustrates the projected density of states (PDOS), showing that the spin-up and spin-down contributions are equal and opposite across the energy spectrum, thereby confirming the persistence of compensated magnetization across

all investigated pressure ranges. The electronic band structure of the HP-II phase reveals a definitive absence of NRSS, as depicted in Fig.3c, aligning with the findings reported by Linnemann *et al.*³¹. Moreover, a large number of band crossings near the Fermi level of the HP-II phase (see Fig.3c) can be attributed to the presence of Weyl points, as previously reported in Ref.³¹.

Alongside modifications in structural and electronic properties, pressure exerts a notable influence on magnetic properties. The magnetic moment (μ) exhibits a decreasing trend with increasing pressure, as illustrated in Table I, aligning well with experimental implication¹⁴. Furthermore, pressure enhances the strength of spin splitting in the valence band, whereas in the conduction band, pressure suppresses the spin splitting (variation of NRSS is illustrated in Fig. 6). This trend is consistent with the findings of Devaraj *et al.*¹¹. Such a trend can be rationalized by examining the projected density of states (PDOS). With increasing pressure, interatomic distances are reduced, which enhances the hybridization between p- and d-orbitals. As a consequence, the contribution of d-orbitals to the conduction band slowly decreases, as shown in Fig. 5¹¹. This decrement in d-orbital character leads to a suppression of non-relativistic spin splitting (NRSS) in the conduction band¹⁵. In contrast, the valence band exhibits the opposite trend: elevated pressure gradually enhances the d-orbital contribution to the valence states, thereby resulting in an enhancement of NRSS. This contrasting behavior highlights the orbital-selective nature of pressure-induced spin splitting and the pivotal role of orbital hybridization in shaping the electronic structure. Furthermore, microscopic parameters are critical in governing the non-relativistic spin splitting (NRSS). In particular, the competition between antiferromagnetic exchange interactions and d-orbital hopping integrals plays a decisive role in modulating NRSS. This relationship can be qualitatively expressed as $|\Delta E| \propto \frac{t_3 t_4}{J}$ ⁶, where t_3 and t_4 correspond to intra-orbital and inter-orbital hopping parameters of the d-orbitals, respectively (within two nearest sublattices), and J denotes the antiferromagnetic exchange energy. Increasing external pressure tends to suppress the magnitude of J , thereby facilitating enhanced electron hopping between orbitals. This results in an effective amplification of the spin splitting¹⁵.

TABLE I. Lattice parameters, unit cell volume (V), magnetic moment per Cr atom (μ_{Cr}), and enthalpy per formula unit (E(eV)/f.u.) for antiferromagnetic CrSb₂ in the marcasite (M) phase under various applied pressures.

P(GPa)	a(Å)	b(Å)	c(Å)	V(Å ³)	μ_{Cr} (μ_B)	E(eV)/f.u.
0	6.026	6.846	3.151	129.991	2.291	-943.528
5	5.951	6.757	3.103	124.774	2.144	-943.383
10	5.894	6.679	3.062	120.539	2.039	-943.242
15	5.843	6.609	3.026	116.853	1.959	-943.106
20	5.797	6.544	2.994	113.579	1.892	-942.974

TABLE II. Lattice parameters, unit cell volume (V), magnetic moment per Cr atom (μ_{Cr}), and enthalpy per formula unit (E(eV)/f.u.) for antiferromagnetic CrSb₂ in the HP-II phase under various applied pressures.

P(GPa)	a(Å)	b(Å)	c(Å)	V(Å ³)	μ_{Cr} (μ_B)	E(eV)/f.u.
0	3.0965	13.056	6.164	249.198	2.678	-943.510
5	3.039	12.882	6.028	235.987	2.309	-943.371
10	2.992	12.689	6.028	228.856	1.928	-943.237
15	2.946	12.516	5.959	219.721	1.555	-943.108
20	2.935	12.378	5.890	213.980	1.248	-942.983

The NRSS can be interpreted using the richer non-relativistic spin group theory, where transformations in spin space and real space can be resolved. This implies that transformations in real space and spin space can act independently. Traditionally, the spin groups are represented by the direct product $r_s \times R_s$ ^{32,33}, where r_s represents transformations in the spin space alone, and R_s (nontrivial spin group) represents a combination of transformations in both real and spin spaces. Three types of nontrivial spin groups describe three magnetic systems, i.e., FM, AFM, and AM⁵⁰. The spin-only group in the case of collinear spins is given by $r_s = C_\infty + \bar{C}_2 C_\infty$ ^{32,33}. C_∞ represents the group containing all the rotational transformations around the common axis of spin. Meanwhile, \bar{C}_2 represents a two-fold rotation around the axis orthogonal to the spin, followed by spin space inversion. The non-trivial spin Laue group that describes the AMs (R_s^{III}) is constructed using isomorphism theorem³³.

$$R_s^{III} = [E||H] + [C_2||G - H]^{50}$$

Here, transformations to the left of the double vertical bars act on spin space, while those to the right act on real space. G denotes the crystallographic Laue group, while H represents its halving subgroup, comprising real-space symmetry operations that map atoms within the same spin sublattice. In contrast, the coset $G - H = AH$ consists of symmetry operations that interchange atoms between opposite spin sublattices⁵⁰. The operator A represents proper or improper, symmorphic or nonsymmorphic rotations. However, unlike in the case of AFMs, the two opposite spin sublattices are not related by translation or inversion symmetry. Now $[C_2||AH]\mathcal{E}(\sigma, k) = \mathcal{E}(-\sigma, k')$, thereby giving rise to a spin-split band structure⁵⁰. For instance, non non-trivial spin Laue group R_s^{III} that characterizes altermagnetism in CrSb₂ is

$$^2m^2m^1m = [E||2/m] + [C_2||C_{2y}][E||2/m]$$

The opposite spin sublattices are related by a non-symmorphic rotation, specifically a twofold rotation (C_2) in spin space around an axis orthogonal to the common spin axis, and a twofold rotation (C_{2y}) in real space around the Y-axis (shown in Fig.??c), followed by

a half-unit-cell translation. The same symmetry classification has been used to discuss NRSS in La_2CuO_4 ⁵⁰ and FeSb_2 ³⁶. Further analysis of the symmetry in CrSb_2 ($Pnnm$ space group) reveals the following combination of operations:

$$\{E, P, M_z, C_{2z}\} + t\mathcal{T}\{C_{2x}, M_x, C_{2y}, M_y\}^{36}$$

Here, the operation \mathcal{T} reverses the spin quantization axis^{32,33,50} and serves as the non-relativistic analog of time-reversal symmetry. The symmetry elements (E, P, C_{2z}, M_z) map each magnetic sublattice onto itself and are classified as symmorphic operations. In contrast, the remaining operations, when combined with the translation t (half-a-unit cell in the case CrSb_2), form nonsymmorphic elements such as glide planes and screw axes. For example

$$\mathcal{T}M_x E(k_x, k_y, k_z, \uparrow) = E(-k_x, k_y, k_z, \downarrow)$$

For $k_x = 0$ (nodal plane), spin up and down bands are degenerate, which corresponds to $\Gamma(0,0,0)$ and $Z(0,0,1/2)$ high symmetry points in Fig.3(a,b). The presence of such symmetry operation results in alternating spin-splitting along $M'-\Gamma-M$ [see Fig.3(a,b)] and $A-Z-A'$ high symmetry paths.

To investigate the dynamical stability of the relaxed structure, we computed the phonon dispersion curves at 0 and 10 GPa for the M-AFM phase (refer to the supplementary material, Figure S2). The absence of negative frequencies confirms the dynamical stability of the structure. With increasing pressure, a significant blue shift is observed in the phonon spectrum across both the acoustic and optical branches. From the phonon density of states, it is evident that the heavier Sb atoms dominate the low-frequency region, whereas the comparatively lighter Cr atoms contribute predominantly to the high-frequency region.

IV. CONCLUSION

We have performed the first-principles DFT calculation to study the structural, electronic, and magnetic properties of CrSb_2 under applied pressure. Our study predicts the structural phase transition from marcasite to HP-II structure at ~ 11.5 GPa. The experimental results

from the temperature-dependent magnetic susceptibility calculation confirm the ground state AFM configuration. The presence of collinear AFM and NRSS of $\sim 0.5\text{eV}$ from the first-principles calculation supports CrSb_2 as a strong altermagnet candidate. Interestingly, we have observed a decrease in the NRSS band around the Fermi level and eventually diminishes above ~ 10 GPa in the HP-II phase, resulting in the flipping of the magnetic characteristic from Altermagnet to conventional AFM. The precise momentum-space positioning of this altermagnetic band splitting holds notable implications for spintronic applications, particularly in enabling the generation of spin-polarized currents in AFMs. Our theoretical findings position CrSb_2 as a compelling candidate for experimental exploration within the emerging framework of altermagnetism. Probing techniques such as anomalous Hall conductivity and magneto-optical Kerr effect (MOKE) measurements may offer critical insights into the symmetry-breaking mechanisms, particularly the violation of time-reversal symmetry (\mathcal{T}) in this material.

ACKNOWLEDGMENTS

RT acknowledges the University Grants Commission (UGC), India, for the Junior Research Fellowship (JRF), ID No. 231620066332.

AUTHOR CONTRIBUTIONS

R. Tamang: Formal analysis, Visualization, Validation, Literature review, Writing-original draft, writing-review & editing.

Shivraj Gurung: Formal analysis, Visualization, Validation, writing-review & editing.

Shalika Ram bhandari: Formal analysis, Visualization, Validation, writing-review & editing.

Matthew J. Stitz: Supervision, Formal analysis, Visualization, Validation, writing-review & editing.

Ganesh Pokharel: Formal analysis, Visualization, Validation, writing-review & editing.

Keshav Shrestha: Formal analysis, Visualization, Validation, writing-review & editing.

D. P. Rai: Project management, Supervision, Resources, software, Formal analysis, Visualization, Validation, writing-review & editing.

¹ H Bai, YC Zhang, YJ Zhou, P Chen, CH Wan, L Han, WX Zhu, SX Liang, YC Su, XF Han, et al. Efficient spin-to-charge conversion via altermagnetic spin splitting effect in antiferromagnet ruo 2. *Physical review letters*, 130(21):216701, 2023.

² Hua Bai, Lei Han, XY Feng, YJ Zhou, RX Su, Qian Wang, LY Liao, WX Zhu, XZ Chen, Feng Pan, et al. Observation of spin splitting torque in a collinear antiferromagnet ruo 2. *Physical Review Letters*, 128(19):197202, 2022.

³ Ling Bai, Wanxiang Feng, Siyuan Liu, Libor Šmejkal, Yuriy Mokrousov, and Yugui Yao. Altermagnetism: Ex-

- ploring new frontiers in magnetism and spintronics. *Advanced Functional Materials*, page 2409327, 2024.
- ⁴ Vincent Baltz, A Hoffmann, S Emori, D-F Shao, and T Jungwirth. Emerging materials in antiferromagnetic spintronics. *APL Materials*, 12(3), 2024.
 - ⁵ Vincent Baltz, Aurelien Manchon, M Tsoi, Takahiro Moriyama, T Ono, and Y Tserkovnyak. Antiferromagnetic spintronics. *Reviews of Modern Physics*, 90(1):015005, 2018.
 - ⁶ Sayantika Bhowal and Nicola A Spaldin. Ferroically ordered magnetic octupoles in d-wave altermagnets. *Physical Review X*, 14(1):011019, 2024.
 - ⁷ Arnab Bose, Nathaniel J Schreiber, Rakshit Jain, Ding-Fu Shao, Hari P Nair, Jiaxin Sun, Xiyue S Zhang, David A Muller, Evgeny Y Tsymbal, Darrell G Schlom, et al. Tilted spin current generated by the collinear antiferromagnet ruthenium dioxide. *Nature Electronics*, 5(5):267–274, 2022.
 - ⁸ Atasi Chakraborty, Rafael González Hernández, Libor Šmejkal, and Jairo Sinova. Strain-induced phase transition from antiferromagnet to altermagnet. *Physical Review B*, 109(14):144421, 2024.
 - ⁹ Boyuan Chi, Leina Jiang, Yu Zhu, Guoqiang Yu, Caihua Wan, Jia Zhang, and Xiufeng Han. Crystal-facet-oriented altermagnets for detecting ferromagnetic and antiferromagnetic states by giant tunneling magnetoresistance. *Physical Review Applied*, 21(3):034038, 2024.
 - ¹⁰ Sachchidanand Das, Dhavala Suri, and Abhiram Soori. Transport across junctions of altermagnets with normal metals and ferromagnets. *Journal of Physics: Condensed Matter*, 35(43):435302, 2023.
 - ¹¹ Nayana Devaraj, Anumita Bose, and Awadhesh Narayan. Interplay of altermagnetism and pressure in hexagonal and orthorhombic mnte. *Physical Review Materials*, 8(10):104407, 2024.
 - ¹² Jianyang Ding, Zhicheng Jiang, Xiuhua Chen, Zicheng Tao, Zhengtai Liu, Tongrui Li, Jishan Liu, Jianping Sun, Jinguang Cheng, Jiayu Liu, et al. Large band splitting in g-wave altermagnet crsb. *Physical Review Letters*, 133(20):206401, 2024.
 - ¹³ Qianheng Du, Huixia Fu, Junzhang Ma, A Chikina, M Radovic, Binghai Yan, and C Petrovic. Surface conductivity in antiferromagnetic semiconductor crsb 2. *Physical Review Research*, 2(4):043085, 2020.
 - ¹⁴ Emma Ehrenreich-Petersen, Mads F Hansen, Justin Jeanneau, Davide Ceresoli, Francesca Menescardi, Martin Ottesen, Vitali Prakapenka, Sergey N Tkachev, and Martin Bremholm. Seven-coordinated high-pressure phase of crsb2 and experimental equation of state of m sb2 (m= cr, fe, ru, os). *Inorganic Chemistry*, 62(31):12203–12212, 2023.
 - ¹⁵ Zhenyu Fan, Zhengming Zhang, Hongchang Wang, Jianhu Gong, Dunhui Wang, and Baomin Wang. High-pressure modulation of altermagnetism in mnf2. *Applied Physics Letters*, 126(8), 2025.
 - ¹⁶ Zexin Feng, Xiaorong Zhou, Libor Šmejkal, Lei Wu, Zengwei Zhu, Huixin Guo, Rafael González-Hernández, Xiaoning Wang, Han Yan, Peixin Qin, et al. An anomalous hall effect in altermagnetic ruthenium dioxide. *Nature Electronics*, 5(11):735–743, 2022.
 - ¹⁷ Paolo Giannozzi, Oliviero Andreussi, Thomas Brumme, Oana Bunau, M Buongiorno Nardelli, Matteo Calandra, Roberto Car, Carlo Cavazzoni, Davide Ceresoli, Matteo Cococcioni, et al. Advanced capabilities for materials modelling with quantum espresso. *Journal of physics: Condensed matter*, 29(46):465901, 2017.
 - ¹⁸ Paolo Giannozzi, Stefano Baroni, Nicola Bonini, Matteo Calandra, Roberto Car, Carlo Cavazzoni, Davide Ceresoli, Guido L Chiarotti, Matteo Cococcioni, Ismaila Dabo, et al. Quantum espresso: a modular and open-source software project for quantum simulations of materials. *Journal of physics: Condensed matter*, 21(39):395502, 2009.
 - ¹⁹ Paolo Giannozzi, Oscar Basergio, Pietro Bonfà, Davide Brunato, Roberto Car, Ivan Carnimeo, Carlo Cavazzoni, Stefano De Gironcoli, Pietro Delugas, Fabrizio Ferrari Ruffino, et al. Quantum espresso toward the exascale. *The Journal of chemical physics*, 152(15), 2020.
 - ²⁰ RD Gonzalez Betancourt, Jan Zubáč, R Gonzalez-Hernandez, Kevin Geishendorf, Zbynek Šobán, Gunther Springholz, Kamil Olejník, Libor Šmejkal, Jairo Sinova, Tomas Jungwirth, et al. Spontaneous anomalous hall effect arising from an unconventional compensated magnetic phase in a semiconductor. *Physical Review Letters*, 130(3):036702, 2023.
 - ²¹ Rafael González-Hernández, Libor Šmejkal, Karel Vybírný, Yuta Yahagi, Jairo Sinova, Tomáš Jungwirth, and Jakub Železný. Efficient electrical spin splitter based on nonrelativistic collinear antiferromagnetism. *Physical Review Letters*, 126(12):127701, 2021.
 - ²² Yaqian Guo, Hui Liu, Oleg Janson, Ion Cosma Fulga, Jeroen van den Brink, and Jorge I Facio. Spin-split collinear antiferromagnets: A large-scale ab-initio study. *Materials Today Physics*, 32:100991, 2023.
 - ²³ Hans Holseth, Arne Kjekshus, Arne F Andresen, Lothar Schäfer, and Akira Shimizu. Compounds with the marcasite type crystal structure. vi. neutron diffraction studies of crsb2 and fesb2. *Acta Chemica Scandinavica*, 24:3309–3316, 1970.
 - ²⁴ Yuan-Yuan Jiang, Zi-An Wang, Kartik Samanta, Shu-Hui Zhang, Rui-Chun Xiao, WJ Lu, YP Sun, Evgeny Y Tsymbal, and Ding-Fu Shao. Prediction of giant tunneling magnetoresistance in ru o 2/ti o 2/ru o 2 (110) antiferromagnetic tunnel junctions. *Physical Review B*, 108(17):174439, 2023.
 - ²⁵ Shutaro Karube, Takahiro Tanaka, Daichi Sugawara, Naohiro Kadoguchi, Makoto Kohda, and Junsaku Nitta. Observation of spin-splitting torque in collinear antiferromagnetic ruo 2. *Physical review letters*, 129(13):137201, 2022.
 - ²⁶ KP Kluczyk, K Gas, MJ Grzybowski, P Skupiński, MA Borysiewicz, T Faş, J Suffczyński, JZ Domagala, K Graszka, A Mycielski, et al. Coexistence of anomalous hall effect and weak magnetization in a nominally collinear antiferromagnet mnte. *Physical Review B*, 110(15):155201, 2024.
 - ²⁷ G Kuhn, S Mankovsky, H Ebert, M Regus, and Wolfgang Bensch. Electronic structure and magnetic properties of crsb 2 and fesb 2 investigated via ab initio calculations. *Physical Review B—Condensed Matter and Materials Physics*, 87(8):085113, 2013.
 - ²⁸ Suyoung Lee, Sangjae Lee, Saegyeol Jung, Jiwon Jung, Donghan Kim, Yeonjae Lee, Byeongjun Seok, Jaeyoung Kim, Byeong Gyu Park, Libor Šmejkal, et al. Broken kramers degeneracy in altermagnetic mnte. *Physical Review Letters*, 132(3):036702, 2024.
 - ²⁹ Miina Leiviskä, Javier Rial, Antonín Bad’ura, Rafael Lopes Seeger, Ismaila Kounta, Sebastian Beckert, Dominik Kriegner, Isabelle Joumard, Eva Schmoranzarová, Jairo Sinova, et al. Anisotropy of the anomalous hall effect in thin films of the altermagnet candidate mn 5 si 3. *Physical Review B*, 109(22):224430, 2024.

- ³⁰ Chen Li, Ke Liu, Shang Peng, Qi Feng, Dequan Jiang, Ting Wen, Hong Xiao, Binbin Yue, and Yonggang Wang. Rewritable pressure-driven n-p conduction switching in marcasite-type crsb2. *Chemistry of Materials*, 35(3):1449–1457, 2023.
- ³¹ Carl Jonas Linnemann, Emma Ehrenreich-Petersen, Davide Ceresoli, Timofey Fedotenko, Innokenty Kantor, Mads Ry Vogel Jørgensen, and Martin Bremholm. Weyl semimetallic phase in high pressure crsb2 and structural compression studies of its high pressure polymorphs. *Journal of Alloys and Compounds*, 1003:175457, 2024.
- ³² Daniel B Litvin. Spin point groups. *Acta Crystallographica Section A: Crystal Physics, Diffraction, Theoretical and General Crystallography*, 33(2):279–287, 1977.
- ³³ Daniel B Litvin and W Opechowski. Spin groups. *Physica*, 76(3):538–554, 1974.
- ³⁴ Fangqi Liu, Zhenhua Zhang, Xiaojuan Yuan, Yong Liu, Sicong Zhu, Zhihong Lu, and Rui Xiong. Giant tunneling magnetoresistance in insulated altermagnet/ferromagnet junctions induced by spin-dependent tunneling effect. *Physical Review B*, 110(13):134437, 2024.
- ³⁵ Igor Mazin and PRX Editors. Altermagnetism—a new punch line of fundamental magnetism, 2022.
- ³⁶ Igor I Mazin, Klaus Koepernik, Michelle D Johannes, Rafael González-Hernández, and Libor Šmejkal. Prediction of unconventional magnetism in doped fcsb2. *Proceedings of the National Academy of Sciences*, 118(42):e2108924118, 2021.
- ³⁷ Makoto Naka, Satoru Hayami, Hiroaki Kusunose, Yuki Yanagi, Yukitoshi Motome, and Hitoshi Seo. Spin current generation in organic antiferromagnets. *Nature communications*, 10(1):4305, 2019.
- ³⁸ Makoto Naka, Yukitoshi Motome, and Hitoshi Seo. Perovskite as a spin current generator. *Physical Review B*, 103(12):125114, 2021.
- ³⁹ K Nakagawa, M Kimata, T Yokouchi, and Y Shiomi. Surface anisotropic magnetoresistance in the antiferromagnetic semiconductor cr sb 2. *Physical Review B*, 107(18):L180405, 2023.
- ⁴⁰ John P Perdew, Adrienn Ruzsinszky, Gabor I Csonka, Oleg A Vydrov, Gustavo E Scuseria, Lucian A Constantin, Xiaolan Zhou, and Kieron Burke. Generalized gradient approximation for solids and their surfaces. *arXiv preprint arXiv:0707.2088*, 2007.
- ⁴¹ Cole Phillips, Ganesh Pokharel, Kyryl Shtefienko, Shalika R Bhandari, David E Graf, DP Rai, and Keshav Shrestha. Electronic structure of the altermagnet candidate fcsb 2: High-field torque magnetometry and density functional theory studies. *Physical Review B*, 111(7):075141, 2025.
- ⁴² Paolo G Radaelli. Tensorial approach to altermagnetism. *Physical Review B*, 110(21):214428, 2024.
- ⁴³ Helena Reichlova, Rafael Lopes Seeger, Rafael González-Hernández, Ismaila Kounta, Richard Schlitz, Dominik Kriegner, Philipp Ritzinger, Michaela Lammel, Miina Leiviskä, Anna Birk Hellenes, et al. Observation of a spontaneous anomalous hall response in the mn5si3 d-wave altermagnet candidate. *Nature Communications*, 15(1):4961, 2024.
- ⁴⁴ Sonka Reimers, Lukas Odenbreit, Libor Šmejkal, Vladimir N Strocov, Procopios Constantinou, Anna B Hellenes, Rodrigo Jaeschke Ubierno, Warley H Campos, Venkata K Bharadwaj, Atasi Chakraborty, et al. Direct observation of altermagnetic band splitting in crsb thin films. *Nature Communications*, 15(1):2116, 2024.
- ⁴⁵ Brian C Sales, Andrew F May, Michael A McGuire, Matthew B Stone, David J Singh, and David Mandrus. Transport, thermal, and magnetic properties of the narrow-gap semiconductor crsb 2. *Physical Review B—Condensed Matter and Materials Physics*, 86(23):235136, 2012.
- ⁴⁶ Ding-Fu Shao, Shu-Hui Zhang, Ming Li, Chang-Beom Eom, and Evgeny Y Tsybal. Spin-neutral currents for spintronics. *Nature Communications*, 12(1):7061, 2021.
- ⁴⁷ Libor Šmejkal, Rafael González-Hernández, Tomáš Jungwirth, and Jairo Sinova. Crystal time-reversal symmetry breaking and spontaneous hall effect in collinear antiferromagnets. *Science advances*, 6(23):eaaz8809, 2020.
- ⁴⁸ Libor Šmejkal, Anna Birk Hellenes, Rafael González-Hernández, Jairo Sinova, and Tomas Jungwirth. Giant and tunneling magnetoresistance in unconventional collinear antiferromagnets with nonrelativistic spin-momentum coupling. *Physical Review X*, 12(1):011028, 2022.
- ⁴⁹ Libor Šmejkal, Alberto Marmodoro, Kyo-Hoon Ahn, Rafael González-Hernández, Ilya Turek, Sergiy Mankovsky, Hubert Ebert, Sunil W D’Souza, Ondřej Šipr, Jairo Sinova, et al. Chiral magnons in altermagnetic ruo 2. *Physical Review Letters*, 131(25):256703, 2023.
- ⁵⁰ Libor Šmejkal, Jairo Sinova, and Tomas Jungwirth. Beyond conventional ferromagnetism and antiferromagnetism: A phase with nonrelativistic spin and crystal rotation symmetry. *Physical Review X*, 12(3):031042, 2022.
- ⁵¹ Libor Šmejkal, Jairo Sinova, and Tomas Jungwirth. Emerging research landscape of altermagnetism. *Physical Review X*, 12(4):040501, 2022.
- ⁵² Cheng Song, Hua Bai, Zhiyuan Zhou, Lei Han, Helena Reichlova, J Hugo Dil, Junwei Liu, Xianzhe Chen, and Feng Pan. Altermagnets as a new class of functional materials. *Nature Reviews Materials*, pages 1–13, 2025.
- ⁵³ Hirotugu Takizawa, Kyota Uheda, and Tadashi Endo. A new ferromagnetic polymorph of crsb2 synthesized under high pressure. *Journal of alloys and compounds*, 287(1-2):145–149, 1999.
- ⁵⁴ R Tamang, Shivraj Gurung, DP Rai, Samy Brahimi, and Samir Lounis. Newly discovered magnetic phase: A brief review on altermagnets. *arXiv preprint arXiv:2412.05377*, 2024.
- ⁵⁵ Teresa Tschirner, Philipp Kefler, Ruben Dario Gonzalez Betancourt, Tommy Kotte, Dominik Kriegner, Bernd Büchner, Joseph Dufouleur, Martin Kamp, Vedran Jovic, Libor Smejkal, et al. Saturation of the anomalous hall effect at high magnetic fields in altermagnetic ruo2. *APL Materials*, 11(10), 2023.
- ⁵⁶ Guowei Yang, Zhanghuan Li, Sai Yang, Jiyuan Li, Hao Zheng, Weifan Zhu, Ze Pan, Yifu Xu, Saizheng Cao, Wenxuan Zhao, et al. Three-dimensional mapping and electronic origin of large altermagnetic splitting near fermi level in crsb. *arXiv preprint arXiv:2405.12575*, 2024.
- ⁵⁷ Guowei Yang, Zhanghuan Li, Sai Yang, Jiyuan Li, Hao Zheng, Weifan Zhu, Ze Pan, Yifu Xu, Saizheng Cao, Wenxuan Zhao, et al. Three-dimensional mapping of the altermagnetic spin splitting in crsb. *Nature Communications*, 16(1):1442, 2025.
- ⁵⁸ Yichi Zhang, Hua Bai, Lei Han, Chong Chen, Yongjian Zhou, Christian H Back, Feng Pan, Yuyan Wang, and Cheng Song. Simultaneous high charge-spin conversion efficiency and large spin diffusion length in altermagnetic ruo2. *Advanced Functional Materials*, 34(24):2313332, 2024.

2024.

- ⁵⁹ Zhiyuan Zhou, Xingkai Cheng, Mengli Hu, Ruiyue Chu, Hua Bai, Lei Han, Junwei Liu, Feng Pan, and Cheng Song. Manipulation of the altermagnetic order in crsb via crystal symmetry. *Nature*, pages 1–6, 2025.
- ⁶⁰ Yu-Peng Zhu, Xiaobing Chen, Xiang-Rui Liu, Yuntian Liu, Pengfei Liu, Heming Zha, Gexing Qu, Caiyun Hong, Jiayu Li, Zhicheng Jiang, et al. Observation of plaid-like spin splitting in a noncoplanar antiferromagnet. *Nature*, 626(7999):523–528, 2024.